Fang, Yunhao et al.

Article

Performance evaluation on multi-scenario urban ventilation corridors based on least cost path

Journal of Urban Management

Provided in Cooperation with:
Chinese Association of Urban Management (CAUM), Taipei

Suggested Citation: Fang, Yunhao et al. (2021) : Performance evaluation on multi-scenario urban ventilation corridors based on least cost path, Journal of Urban Management, ISSN 2226-5856, Elsevier, Amsterdam, Vol. 10, Iss. 1, pp. 3-15, https://doi.org/10.1016/j.jum.2020.06.006

This Version is available at:
https://hdl.handle.net/10419/271409

Journal of Urban Management 10 (2021) 3–15

HOSTED BY

Contents lists available at ScienceDirect

Journal of Urban Management

journal homepage: www.elsevier.com/locate/jum

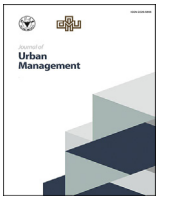

Research Article

Performance evaluation on multi-scenario urban ventilation corridors based on least cost path

Yunhao Fang [a], Kangkang Gu [a,b,*], Zhao Qian [a], Zhen Sun [a], Yongzheng Wang [a], Ai Wang [a]

[a] School of Architecture & Planning, Anhui Jianzhu University, Hefei, 230022, China
[b] Collaborative Innovation Center of Urbanization Construction in Anhui Province, Hefei, China

ARTICLE INFO

Keywords:
Ventilation corridor
Vegetated areas
Waters
Least cost path (LCP)
Heat island effect

ABSTRACT

Ventilation Corridor is an important technique to mitigate local climate problems. Evaluating the benefits of ventilation corridors has gradually become the standard of its construction in cities. Previous studies have often analyzed the volume of ventilation from the perspective of geometric morphology, while there is a lack of discussion on its performance. Therefore, this study innovatively combined the roughness length (Z_0), 3-dimensional aerodynamics parameter, with NDVI and M-NDWI, 2-dimensional indices of land cover through the combination of remote sensing inversion and urban morphology analysis. Compared with the traditional ventilation method, the composite indicator could not only guarantee ventilation volume, but also consider the cooling benefits brought by waters and vegetated areas. In detail, this study was contextualized in four districts in the city core of Hefei, Anhui Province, China. Based on the method of least cost path, we set up four different schemes for comparison, including roughness, roughness + vegetated areas, roughness + waters, and roughness + vegetated areas + waters. Comparative results were effectively verified through land surface temperature retrieved from the Landsat Thematic Mapper. Results were as follows: (1) Different scenarios exerted different impacts on urban ventilation. Of the four regions, the ventilation corridor that only considers Z_0 presented the highest average land surface temperature. (2) The general temperature of ventilation corridors along the path of Z_0 + NDVI + M-NDWI was respectively 34.11 °C, 31.73 °C, 34.80 °C, and 34.93 °C, presenting a lowest temperature compared with other scenarios of the same region. (3) Among the four regions, ventilation corridors constructed based on the path of Z_0 + M-NDWI presented a slightly lower temperature that those based on Z_0+NDVI, with respective data of 34.22 °C < 34.55 °C, 31.85 °C < 31.91 °C, 34.81 °C < 34.82 °C, and 35.21 °C < 35.38 °C. The results provided methods and evidence for performance evaluation on urban land surface ventilation corridors.

1. Introduction

Traditional modifications of city structures and anthropogenic pollution have significantly altered the climate in urban areas. For instance, the phenomenon that urbanized areas suffer from warmer temperatures than their neighboring rural or suburban areas is known as urban heat island (UHI) (Oke, 1982; He et al., 2019). Optimal urban ventilation can enhance air flow capacity and reduce building energy consumption in the summer, which plays an important role in alleviating the urban heat island effect (Hong & Lin,

* Corresponding author. School of Architecture & Planning, Anhui Jianzhu University, Hefei, 230022, China.
E-mail address: kangkanggu@163.com (K. Gu).

https://doi.org/10.1016/j.jum.2020.06.006
Received 22 February 2020; Received in revised form 27 May 2020; Accepted 20 June 2020
Available online 28 August 2020

2015; Coccolo et al., 2016). Thus, the urban ventilation has been emphasized in practice and classified into key schemes of urban planning (Luo et al., 2017). However, actual urban planning often does not consider the efficiency of urban ventilation, which means that airflow cannot guarantee its effectiveness in mitigating climate issues such as the heat island effect (Cariolet et al., 2018; Yuan et al., 2014).

Urban morphology has been applied to explain urban climate change, which is also important for urban ventilation efficiency (Edussuriya et al., 2011; Stewart & Oke, 2012). Low horizontal wind speed is usually associated with high surface roughness, as the energy would be lost by vertical instability due to a high building density (Huang et al., 2014). The pressure difference along temperature gradients can also cause low-level breezes across the urban-rural boundary (Wong et al., 2010). In the previous studies, most data included in urban ventilation were from ground level instruments. The gathering of data over large regions such as a city, therefore, was a major challenge to these studies (Hang et al., 2012; Liu et al., 2019; Vernay et al., 2015). Currently, computer numerical simulation approaches such as computational fluid dynamics (CFD) are applied to analyze urban ventilation efficiency (Ding et al., 2017; Lyu et al., 2015). Specifically, it comprises a set of physical models which attempt to closely match the real urban geometry and thus simulate the air flow around buildings and along streets. The wind pressure and velocity are analyzed to provide feedback on the wind environment (Bajsanski et al., 2016; Guo et al., 2015; Hsieh & Huang, 2016). However, these simulations mostly focus strongly on the physical environment of some districts and buildings that cover small ranges (Badas et al., 2017). Therefore, for urban scale calculations, especially over densely urbanized regions with complex building structures, it is difficult to estimate ventilation efficiency.

The development of Geographic Information System (GIS) and remote sensing technology filled this gap (Yim et al., 2014). In addition, the mathematical model can simplify surface conditions by estimating roughness parameters of building structures (Li et al., 2019a; Wrobel-Niedzwiecka et al., 2019; Wen et al., 2017). Many morphological parameters and diffusion models have been applied to calculate the ground roughness in cities (Burian et al., 2002). The calculation methods include parameters such as building height, building area density, frontal area index, height-to-width ratio, roughness length, and displacement height, etc. Among these urban morphological parameters, the roughness length has been suggested as the most appropriate indicator of the roughness of urban surfaces

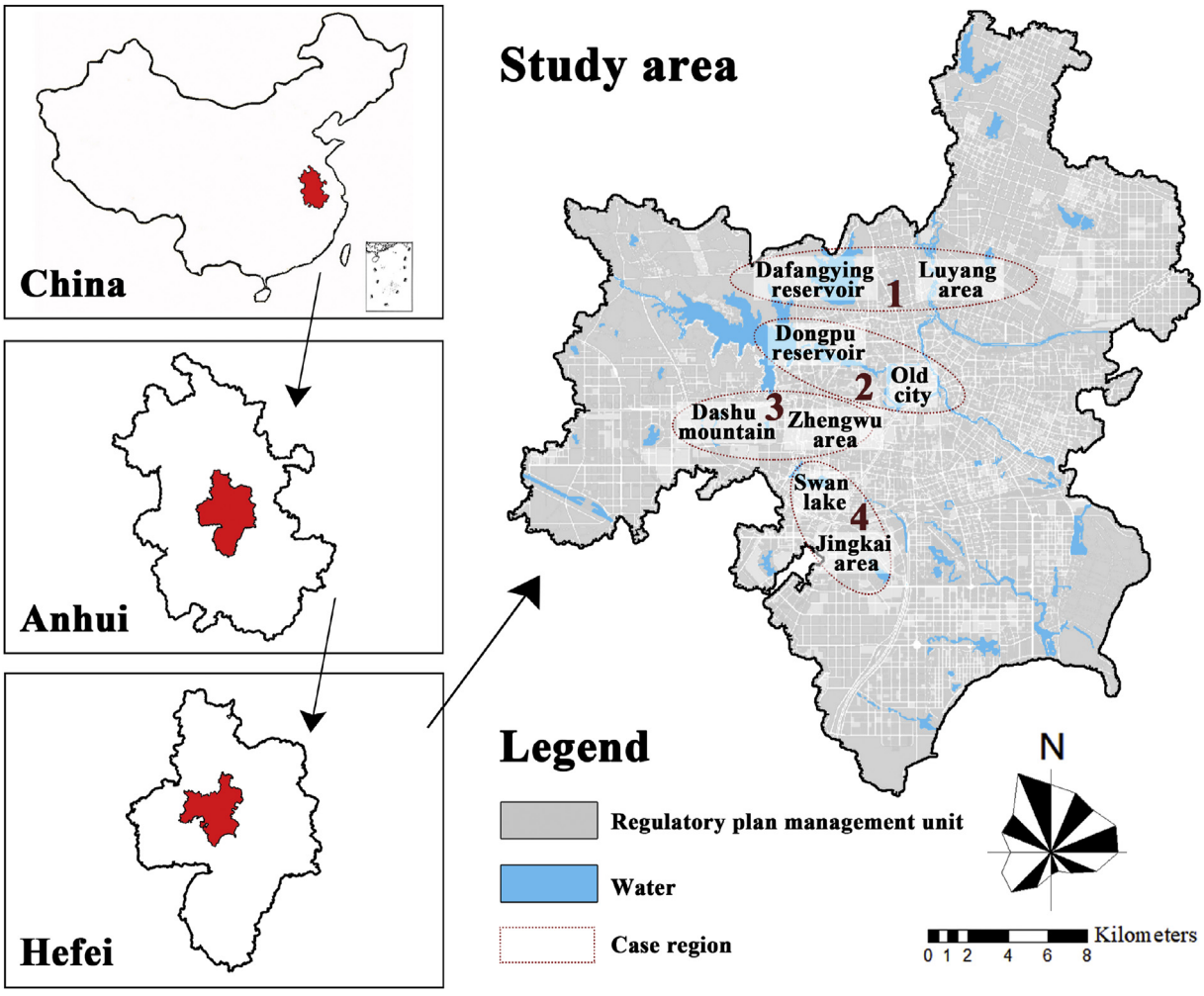

Fig. 1. Research area.

for meso-scale meteorological and urban dispersion models (Kent et al., 2017). Previous studies on urban planning applied a low roughness length to construct ventilation corridors, but the optimal ventilation benefits cannot be achieved by only considering urban morphology (Huang & Wang, 2019; Weng et al., 2015; He et al., 2020a). It is known that vegetated areas and waters have a strong cooling effect (Qiao et al., 2017; Zhang & Li, 2017; He et al., 2020b). As is expressed by the mathematical formula, they have the same low roughness length as road or open space. Specifically, this method can generate strong enough winds to maintain the volume and speed of the moving air, ignoring the benefits of the air temperature.

The purpose of this study is to design ventilation corridors addressing temperature influence according to land cover in order to improve urban ventilation efficiency. Accordingly, by combining 3-dimensional aerodynamics parameter with 2-dimensional indices through remote sensing inversion and the analysis of urban morphology, we chose the main area of Hefei as research object, based on the least cost path (LCP) method, to comprehensively compare the optimization cooling effect of urban vegetated areas and waters on land surface ventilation.

2. Research area and methods

2.1. Research area

Hefei (116°41′E−117°58′E, 30°57′N-32°37′N) locates in the eastern China, the middle latitude zone (Fig. 1). The terrain mostly consists of plains, hills and mountains. It belongs to humid subtropical climate, with distinctive four seasons and an average annual temperature of 15.7 °C. Its average annual precipitation is about 1000 mm, and average relative humidity 77%. An annual mainstream

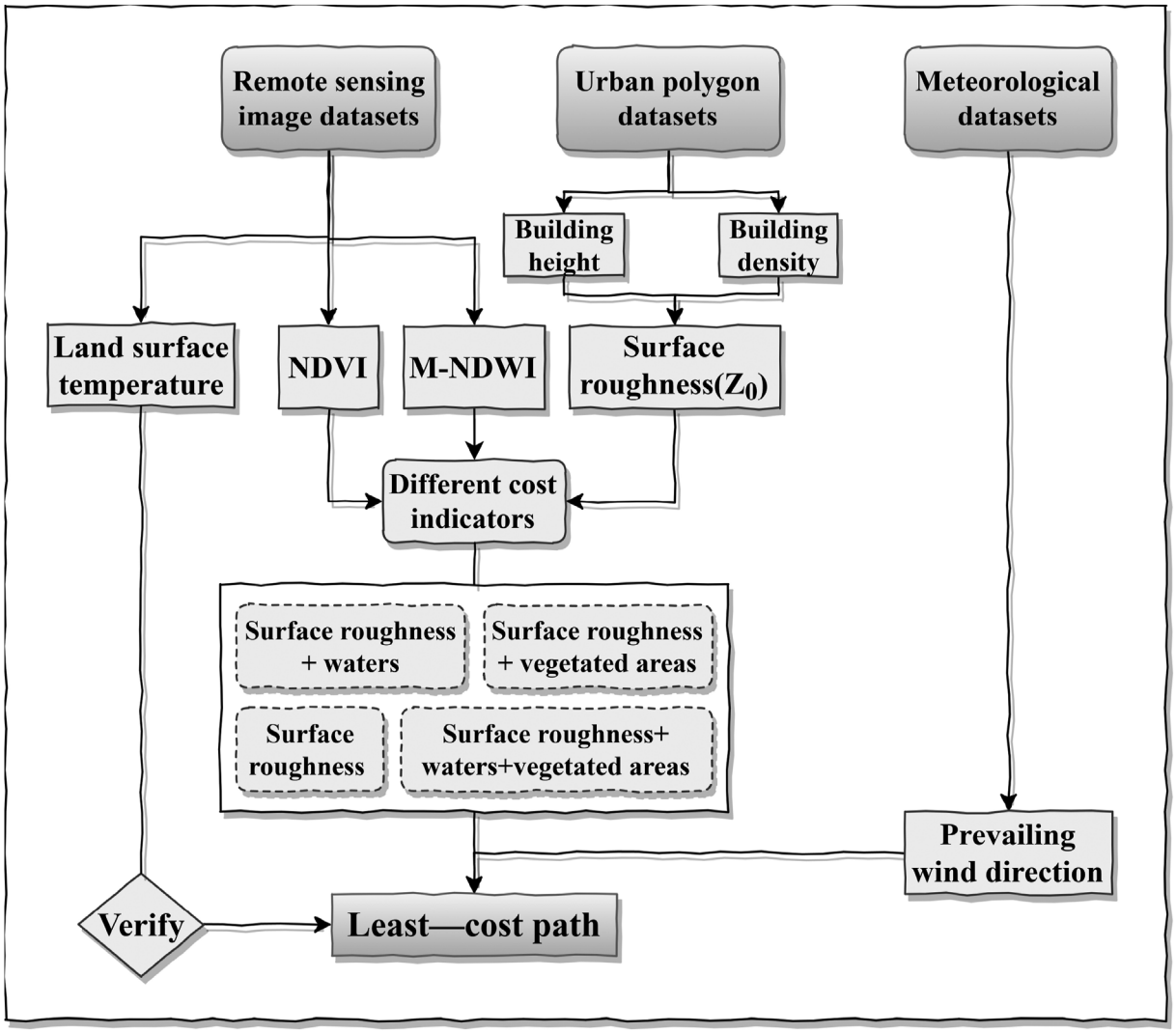

Fig. 2. Research framework.

prevails north and northwest throughout the year. By the end of 2018, Hefei had a resident population of 8.087 million. Meanwhile, farmland in the main urban area is the dominant landscape in this zone, accounting for 63.82%. Water area account for 6.03% and vegetation account for 2.68%. In addition, the construction area reached 460 km^2, accounting for 27.47%. In recent years, due to increasing infrastructure and haze weather, the pullulation of $PM_{2.5}$ increased significantly, and the urban heat island effect exacerbated annually. In Hefei, its heat island effect in winter is more intense than that in summer (Wang et al., 2019). In this study, we simulated and compared four regions in Hefei, which contain both vegetated areas, waters and region center. To be specific, the region 1 covered the Dafangying reservoir and Luyang area, the region 2 contained the Dongpu reservoir and Old city, the region 3 included the Dashu mountain and Zhengwu area, the region 4 covered the Swan Lake area and Jingkai area.

2.2. Research Framework

According to the German theory of ventilation corridor construction, the urban underlying land surface is divided into "the effective space" (Wirkungsraum), "the compensation space" (Ausgleichsraum), and "the ventilation path" (Luftleitbahn) (Liu & Shen, 2010). The effective space refers to area with thermal or air pollution. The compensation space, or say, compensation space for climate ecology, exchanges air with its adjacent space in order to generates regional air circulation. Furthermore, urban natural ventilation gets enhanced, thereby alleviating problems like urban heat island effect and other pollution. The ventilation path connects the effective space to the compensation space, with relatively low land surface roughness and less resistance to air flow (Weng et al., 2015). In this study, 30m*30m grids in Hefei were selected as samples. We calculated the intensity of the heat island using satellite remote sensing data, and identify the effective space and compensation space. In addition, data used in this study also includes Geographic Information System (GIS) data on land cover, and buildings for 2016 and relevant urban planning materials of Hefei. We used these data to analyze the urban wind environment and extract the parameters of urban spatial form. And then we used that data to build up the different costs, including roughness, roughness + vegetated areas, roughness + waters, and roughness + vegetated areas + waters. Then, this study is based on cost to construct urban land surface ventilation corridors between the effective space and compensation space applied LCP as the model to compare the ventilation efficiency of the four models. Finally, remote sensing images were applied to verify the ventilation potential of the four models. The specific process is exhibited in Fig. 2.

2.3. Analysis on least cost path (LCP)

2.3.1. Methods to extract cost index

2.3.1.1. Land surface roughness (Z_0). The roughness elements of urban underlying surface are complicated. Buildings work as resistance collection to ventilation, and thereby affect wind speed. Urban roughness elements and landform resist the flow of currents (Gál & Sümeghy, 2007). Therefore, urban land surface roughness Z_0 could partly reflect the ventilation potential near urban land surface (Bottema, 1997). According to relevant studies, roughness of urban land surface is mainly caused by buildings. Mainly determined by building density and building height (Bottema & Mestayer, 1998). Therefore, in the urban area, this study uses the morphological model to estimate the roughness of urban surface Z_0, including:

$$\frac{Z_d}{Z_h} = 1.0 - \frac{1.0 - \exp\left[-(7.5 \times 2 \times \lambda_F)^{0.5}\right]}{(7.5 \times 2 \times \lambda_F)^{0.5}} \tag{1}$$

$$\frac{Z_0}{Z_h} = \left(1.0 - \frac{Z_d}{Z_h}\right)\exp\left(-0.4 \times \frac{U_h}{u_*} + 0.193\right) \tag{2}$$

$$\frac{u_*}{U_h} = \min\left[(0.003 + 0.3 \times \lambda_F)^{0.5}, 0.3\right] \tag{3}$$

In the equation, Z_d (m) is the height of zero plane displacement; Z_0 (m) is the height of roughness degree; Z_h (m) is the height of building; Z_d/Z_h is the normalized height of zero plane displacement; Z_0/Z_h is the normalized height of roughness degree; U_h is wind speed; u^* is shear velocity; λF is building frontal area, which is closely related to the urban building density λP. In this study, when building density λP concentrates on the area of 0.35, Z_0/Z_h reached the peak. Then the relationship of λF and λP can be generated, that is, $\lambda F = 0.8\lambda P$ (Liu et al., 2017).

2.3.1.2. Normalized difference vegetation index (NDVI) and modified normalized difference water index (M-NDWI). Waters have a lower roughness length than the other land surfaces, which is also the case with the vegetation. This study relies on the ventilation corridors of urban vegetated areas and waters, which can not only ensure a certain amount of ventilation, but also form a blue-green cyberspace to effectively alleviate urban heat island effect. Besides, the two indicators can connect to natural system, purifying spatial pollution from the internal of city, compared with buildings with low roughness. Therefore, we consider the actual situation of Hefei and take vegetated areas and waters into the consideration of cost.

NDVI could accurately reflect the spatial distribution and growth details of plants (Zheng et al., 2018; Formica et al., 2017). M-NDWI performed better in exacting waters than NDWI, as it could better reflect the features and ranges of waters (Ghosh et al., 2015). The both indicators, range from −1 to 1, can effectively reflect the coverage of urban vegetated areas and waters. The larger the index, the higher

the vegetation coverage and water coverage. This study was conducted in main urban area of Hefei, based on Landsat8 OLI/TIRS data, and applied software ENVI5.3 to conduct band calculation after radiation correction. Spatial analysis ArcGIS was then applied to generate NDVI and M-NDWI, which are considered as important weighted indices of urban vegetated areas and waters.

2.3.2. Valuation under different ventilation corridor thresholds

The valuation of ventilation corridor costs is crucial for land surface ventilation corridor construction. Hefei is mainly a plain with an average elevation of 20–40 m, so that can be ignored in the selection of cost. For these reasons, we first apply normalization to each of the considered factors in this study. Specifically, three original variables Z_0, NDVI and M-NDWI were defined from 1 to 10 by using the reclassification Tool of ArcGIS. It is worth noting that the higher the value of Z_0, the higher the cost, while NDVI and M-NDWI represent the opposite, the higher the index value, the lower the cost. Then, for a multi-scene comparison, we not only consider the underlying land surface roughness (Z_0) factor, but also add different impact generated by vegetated areas (NDVI), waters (M-NDWI) and vegetated areas + waters (NDVI + M-NDWI). In this study, Analytic hierarchy process was applied to assess the factors and their accumulated contributions were listed in Table 1. The numerical settings in Table 1 not only take account into that the roughness of the land surface is higher than that of waters and vegetated areas, but also that the land coverage in the city is relatively wide, so the cumulative contribution cannot be too low.

2.3.3. The construction of ventilation corridor by LCP

The construction of ventilation corridor by LCP is to ensure ventilation corridor planning is conducted by path with least wind resistance, and to guarantee the comprehensive benefits of vegetated areas and waters could be truly brought to city. Generally speaking, LCP, as a kind of analytical model, needs to consider the different cost of grid surface to construct ventilation corridor paths. Compared to previous applications, we innovatively considered the selection of the dominant wind direction and the location of the LCP, that is the selection of the effective space and compensation space. This approach ensures maximum cost effectiveness of the ventilation corridors for the study area. The formula for calculating LCP is shown in equation (4) (Li et al., 2019b).

$$LCP = f_{min} \sum_{j=n}^{i=m} (D_{ij} \times R_i) \tag{4}$$

In equation (4), LCP is the minimum of accumulated resistance; D_{ij} is the weight coefficient of resistance factor i in pixel j; R_i is the resistance value to motion of factor i; n and m are the number of the type of source and cost factor.

2.3.4. Confirmation of ventilation efficiency

Heat island intensity is recognized as a significant factor influencing urban ventilation efficiency. The lower the air temperature, the greater the ventilation rate under normal conditions (Marzena et al., 2017; Morakinyo et al., 2013; Yin et al., 2018). But there are exceptions, for instance, the penetration of hot wind (derived from the inland desert area) with high ventilation efficiency results in the enhancement of land surface temperature (He, 2018). It really depends on whether the wind source is cool or not. Therefore, in order to ensure the cooling of the wind source, the study set it in the mountain or waters. Although the air temperature was a good reflection of the urban heat island phenomenon, the temperature measurement was time-consuming and labor-intensive, besides, the measurement range is difficult to cover. Therefore, we used the urban surface land temperature (LST) inversion from the Landsat TM thermal band to validate the ventilation efficiency. Relevant studies show that there is a certain difference between the surface temperature and the air temperature (Rao et al., 2019). In particular, the measurement object and diurnal variation rule of LST and air temperature are different. Despite the numerical differences, there was a strong correlation between LST and air temperature, and LST increased with the increase of air temperature (Sheng et al., 2017). In general, LST can describe the heat island intensity of a city. For the specific conversion method, please refer to formula (7).

According to Landsat8 OLI/TIRS remote sensing data on April 10th, 2018 and atmospheric correction, software ENVI5.3 was applied to conduct inversion on heat island intensity. The temperature generated was then coupled with cost paths to comprehensive analyze the ventilation potential of urban land surface (Marzena & Katarzyna, 2016; Qiao et al., 2017). This method removed the effects of atmospheric radiation on the surface based on real-time atmospheric sounding data to obtain a true ground heat radiation intensity. At the same time the algorithm also considers that the thermal infrared radiation brightness value (L_λ) comprises of the atmospheric upward radiance (L_u), the atmospheric downward radiance (L_d) and the true radiation received by satellite sensor from the ground.

$$L_\lambda = [\varepsilon L_T + (1 - \varepsilon) L_d]\tau + L_u \tag{5}$$

where ε is the surface specific emissivity; L_T is the radiant brightness of a black body with temperature (T (K)) in the thermal infrared band; τ is the atmospheric transmittance, which can be obtained using online values of L_u and L_d (https://atmcorr.Gsfc.nasa.gov/). Based

Table 1
The characteristic value of each principal component and its cumulative contribution rate.

Cost Factors	Land Surface Roughness	Land Surface Roughness + Vegetated Areas		Land Surface Roughness + Waters		Land Surface Roughness + Vegetated Areas + Waters		
Contribution Rate	Z_0	Z_0	NDVI	Z_0	M-NDWI	Z_0	NDVI	M-NDWI
	1	0.40	0.60	0.40	0.60	0.375	0.375	0.25

on the L_T obtained from formula (5), the surface temperature (T_s) was obtained using formula (6). The relevant parameters for each satellite are given in Table 2.

$$T_s = K_2 / ln[1 + K_1 / L_T] \tag{6}$$

The heat island intensity was then calculated using the UHI intensity index (UHII) algorithm, and the UHI scale index formula is shown in formula (7).

$$UHII_i = T_i - \frac{1}{n}\sum_{1}^{n} T_{crop} \tag{7}$$

where $UHII_i$ is the heat island intensity corresponding to the ith pixel on the image; T_i is the surface temperature; n is the number of effective pixels in the suburban farmland; and T_{crop} is the surface temperature in the suburban farmland, which means the average surface temperature of all surrounding agricultural and forest land.

3. Results and analysis

3.1. Spatial distribution features of cost indices

3.1.1. Analysis on land surface roughness

According to results, as is shown in Fig. 3, the general distribution demonstrated “two peaks and multiple bottoms”. To see from different ranges of roughness, Binhu area in the south and a small amount of Zhengwu area had relatively high land surface roughness, distributed in patches, belonging to “two peaks”. The land surface roughness in these areas were basically in the range between 9.09m to 13.95m. Old city and Luyang area in the north ranked the second, scattered in the figure, and the roughness was in the range of 2.79–5.66. The suburbs and part of Forest and Wetland parks had relatively low roughness, belonging to “multiple bottoms”, generally in the range of 0.40–2.79m. In general, roughness in the main urban area of Hefei reached peak in Binhu area in the south and Zhengwu area, and gradually reduced from the inside out.

3.1.2. Analysis on normalized difference vegetation index (NDVI) and modified normalized difference water index (M-NDWI)

It can be seen from spatial distribution (Fig. 4) that NDVI demonstrated the feature of “multiple peaks and two bottoms”. Areas with relatively high index were distributed in the surroundings of Dongpu reservoir and Dafangying reservoir in the northwest of main urban area, as well as Baohe area and Binhu area in the south, mostly in the range of 0.40–0.57. These areas were basically in patches, belonging to peaks of NDVI distribution. Shushan area in the west ranked the second, scattered in the figure. Dongpu reservoir and Dafangying reservoir in the northwest had the lowest index, mainly in the range of −0.20∼-0.01, belonging to “two bottoms”. The index generally rose from the inside out. M-NDWI had the feature of “two peaks and multiple bottoms”. “Two peaks” were in the area of Dongpu reservoir and Dafangying reservoir, with a general index between 0.16–0.35. The others were distributed in main rivers and lakes of the city.

3.2. Analysis on LCP

3.2.1. Overlay analysis on Different Cost Thresholds

In the main urban area of Hefei, based on urban land surface roughness, we respectively discussed the impact of vegetated areas, waters, vegetated areas and waters on ventilation corridors of the city. With the reference group of only considering land surface roughness (Z_0), we constructed three types of urban underlying land surface (roughness, roughness + vegetated areas, roughness + waters, and roughness + vegetated areas + waters). According to the difference of their accumulated contribution, we conducted overlay analysis to respectively generate four cost land surfaces, that is, Z_0, Z_0+M-NDWI, Z_0+NDVI and Z_0+M-NDWI + NDVI, thereby generating the general cost of four research areas, as is shown in Fig. 5.

3.2.2. Ventilation corridor construction by LCP

The ventilation corridor by LCP model can ensure the air flow between effective space and compensation space. In general, the construction of effective space and compensation space are not optional as the source points and destination points of the LCP model. The starting points should be set at the urban cold sources or the upwind of the prevailing wind all year round. The destination points, on the other hand, should be set to downwind of the prevailing wind in the case of dense heat sources in the city. Hefei is the perennial north and northwest direction, so we selected four typical regions and the source and destination points of the least-cost path within the

Table 2
Parameters used in the radiative transfer equation-based method.

Landsat type	K_1/(W/(m^2·sr·μm))	K_2/K
Landsat 5	607.76	1260.56
Landsat 7	666.09	1282.71
Landsat 8	774.89	1321.08

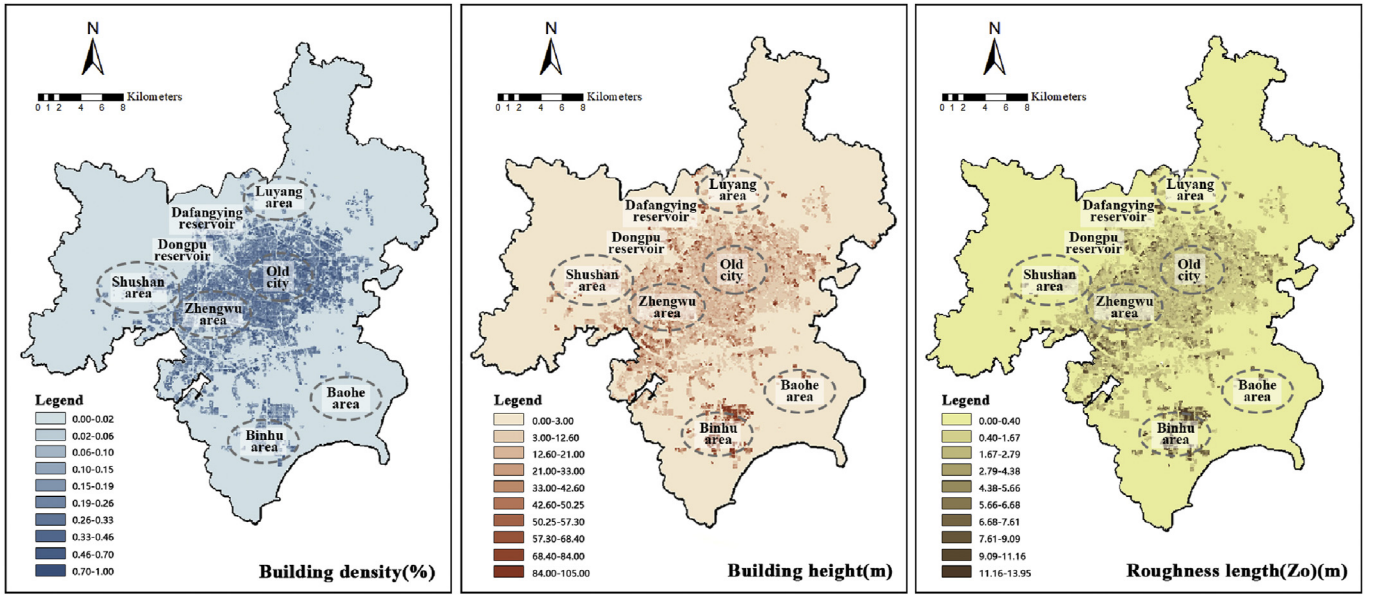

Fig. 3. Spatial Distribution of Density of Building (left), Height of Building (middle) and Land surface Roughness (right).

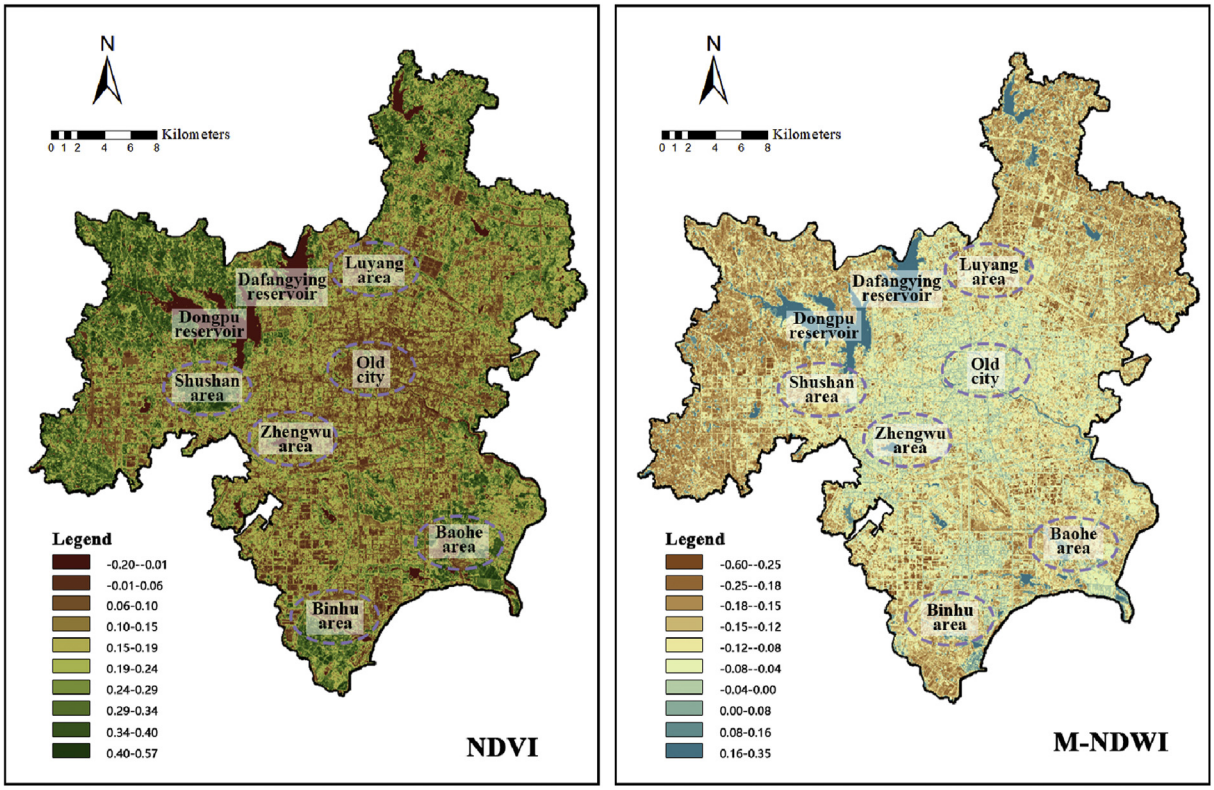

Fig. 4. Spatial distribution of NDVI and M-NDWI

region. Its starting points included Dongpu reservoir, Dafangying reservoir in the northwest, Dashu mountain and Swan Lake area. The destination points are determined in the area with high development intensity near the cold source, including the centers of Luyang area, Old city, Zhengwu area and Jingkai area. According to the sheet layers of different costs, the ventilation corridors constructed in this study are shown in Fig. 6.

Results showed that the general flows of four corridors were almost the same, and no resistance got in the way of north wind or northwest wind. Fresh air could flow from the compensation space through ventilation corridors to the effective space—centers of various main urban areas. However, different ventilation corridors generated different types of land surface paths at the regional level. Among four areas, ventilation corridor A mainly past trunk and secondary trunk roads and squares, consisting of cement and asphalt roads, as well as relatively open underlying land surface like vegetation. Ventilation corridor B mainly past urban green lands like shelter forest area and parks, and a few past non-permeable land surfaces like roads and low-rise buildings. Ventilation corridor C mainly past urban waters like moat, swan lake and reservoirs, and the others flowed to area with low intensity of development. Ventilation corridor D flow through urban natural environments like vegetated areas and waters, as well as artificial environments like buildings.

3.3. Simulation and confirmation

In order to determine the specific influence of ventilation corridors on urban space, constructed by different cost paths, the heat island intensity was used for inversion due to the correlation between the two. In addition, LST was used to represent the heat island intensity in this study because of the high consistency between the LST, obtained by remote sensing image, and weather temperature at that time (Sheng et al., 2017). Therefore, in order to prove different paths of ventilation efficiency, we conducted four cases of coupling ventilation path and surface temperature (Marzena et al., 2017; Qiao et al., 2017), and made statistics on the overlapping pixels in a grid of 30*30, as shown in Fig. 7.

It is indicated in results that heat island intensity of different areas were diversified. In general, it showed the pattern of “two bottoms and multiple peaks” with significant different in temperature. The land surface temperature of the compensation space was obviously lower than that of the effective space. Mountains and waters around the main urban area were generally of low temperature, mostly lower than 18.34 °C. Dongpu reservoir and Dafangying reservoir, located in the northwest of the main urban area, had the lowest temperature, 12.62 °C. And they were the two bottoms in the figure. In the meantime, all regions in the main urban area exhibited generally high temperature, higher than 31.78 °C in general. Peaks were scattered, and Luyang area in the north and Jingkai area in the south had the highest land surface temperature. In general, land surface temperature in the main urban area of Hefei demonstrated a spatial pattern of “cold outside but hot inside”, and temperature was gradually reducing from the inside out.

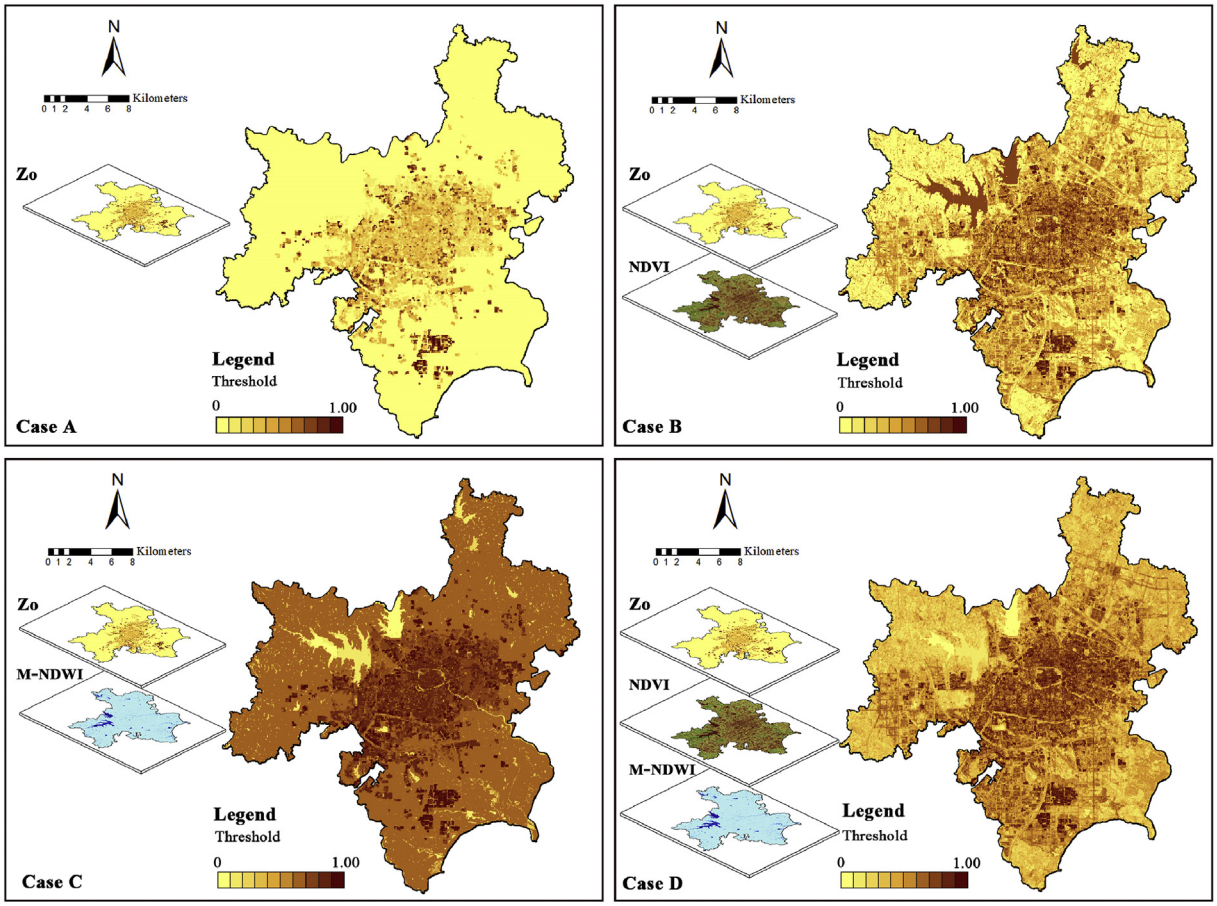

Fig. 5. Spatial distribution of different cost thresholds.

The average land surface temperature of ventilation corridors constructed by different costs in four regions was calculated and analyzed, as shown in Fig. 7 and Table 3. It is obviously that land surface temperature of different regions differed due to spatial distribution. Region 1, 3, and 4 had a generally high temperature, while the ventilation corridors in region 2, between Dongpu reservoir and Dafangying reservoir, had the lowest temperature in general, with an average temperature of 31.93 °C. The highest land surface temperature was in region 4, that is, the ventilation corridors between Swan Lake and Jingkai area, and the average temperature was 35.24 °C. The land surface temperature of the same region was within certain range, but temperature differs in different cases. The largest difference in temperature was in ventilation corridors of region 1, connecting Dafangying reservoir and the center of Luyang area, which was 0.78 °C. In general, whether it is the average comparison of a single region or the average comparison of an entire region, case A had the highest temperature, followed by case B and C, while case D had the lowest temperature.

4. Discussion

A more strategic and integrated process could help to ensure that multiple ventilation corridors are provided to the areas of the city that need them most. Most studies use urban morphology for reference to determine ventilation corridors, lacking of comprehensiveness. So we introduce the remote sensing inversion to improve the delineation of ventilation corridors (He et al., 2020). The method of combining 3-dimensional aerodynamics parameter with 2-dimensional indices was used to evaluate ventilation seeking to steer spatial planning about an integrated roughness length Z_0, NDVI, and M-NDWI. It is consistent with studying the ventilation corridors from a macro perspective, since they have conducted comprehensive research and judgment according to relevant criteria (Li et al., 2019; Marzena et al., 2017). But using different indicators produces different results. Therefore, in this study, in order to further study the rationality of index construction, we need to comprehensively compare the cooling effects of different indicators and their causes in the ventilation corridors. Based on this, we compared four scenarios in the study area. The statistical results of four schemes are shown in Table 3 and Fig. 7.

According to the case A with case B and C, the temperature of the ventilation corridors, constructed with roughness length Z_0, are the highest. In case A, the average temperature of the four regions is 34.37 °C, while in case B and C, the average temperature is 34.17 °C and 34.02 °C, respectively. Specifically, in case A only urban morphology is taken into account in the construction of ventilation corridors,

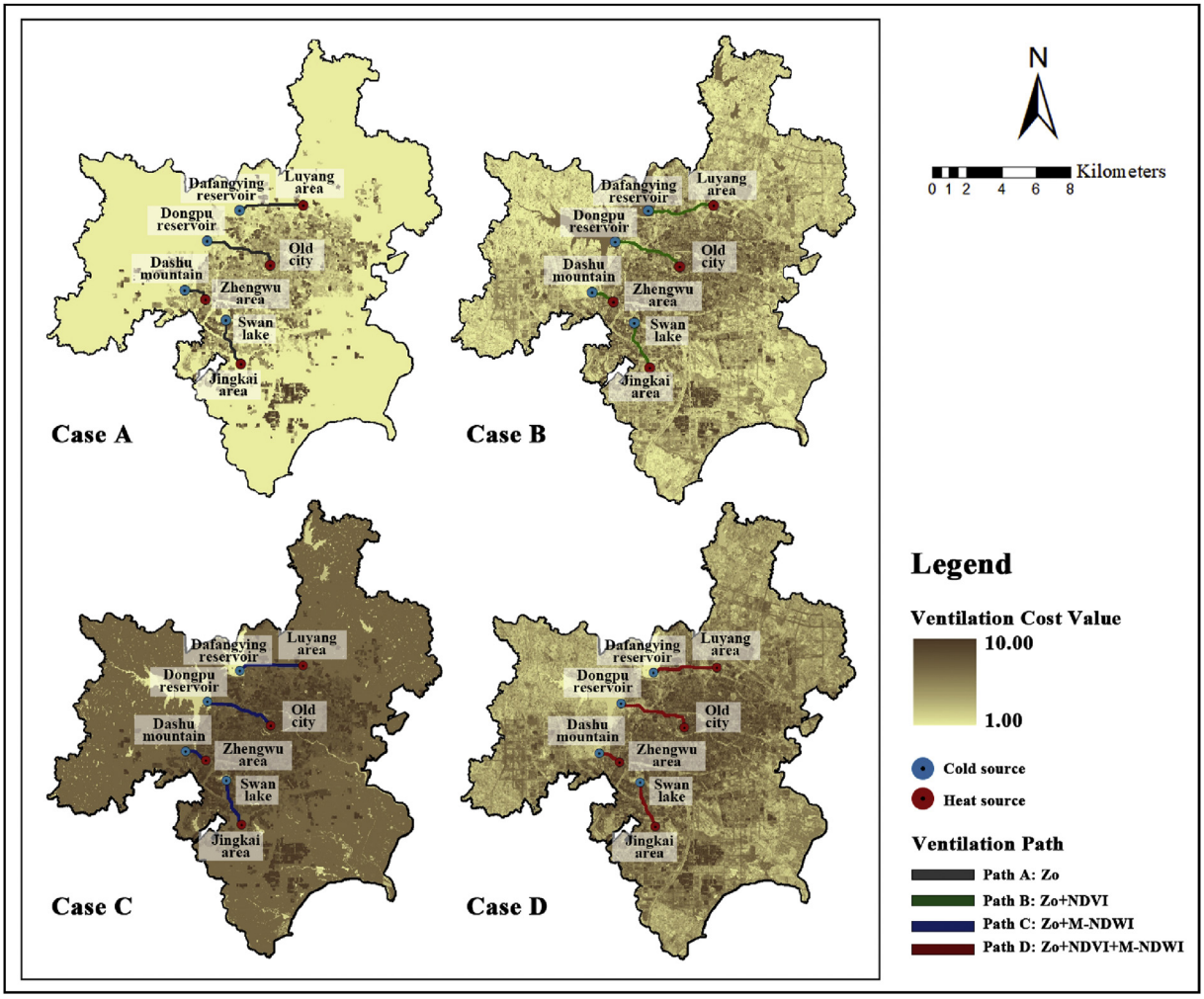

Fig. 6. Distribution of ventilation corridors by LCP

while in case B and case C the study considers the types of underlying land surface through remote sensing images on the basis of urban morphology including vegetated areas and waters. This comparison validates the former studies that the cooling effect of vegetated areas and waters is much greater than the concrete roads and hard paving bricks in cities at the same rough surface length (Li et al., 2013).

In addition, the study also compared case B and case C. As we can be seen from Table 3, the average temperature of each region in case B is not only higher than that of case C, but also the specific temperature in case B, including 34.55 °C, 31.91 °C, 34.82 °C and 35.38 °C, is higher than that of the ventilation corridor of case C in the same region, including 34.22 °C, 31.85 °C, 34.81 °C and 35.21 °C. The main reason for this is that the ventilation corridors of case C mainly passed through waters, while the ventilation corridors of case B mainly passed through vegetated areas. Relevant studies show that the cooling mechanism and cooling intensity of vegetated areas and waters are different in the construction of ventilation corridors. Specifically, waters mainly reduce the temperature of the ventilation corridors by evaporative heat dissipation, which tends to form a significant cold radiation effect on the surroundings, while vegetated areas influence temperature mainly by exchanging with the surrounding air, including photosynthesis and transpiration (Jan et al., 2013). The most important point is that when the wind body flows at a low altitude ($\leq$2m), the thermal mitigation capacity of vegetated areas is lower than the waters (Du, 2018).

Finally, we comprehensively compared the four schemes and found that the ventilation corridors in case D had the lowest average temperature 33.89 °C, showing the ventilation corridors passing through both vegetated areas and waters. Therefore, the combination of vegetated areas and waters can make up for the cooling area of the underlying land surface of the city in space and bring relatively cooling air to the surface of the city. In addition, related studies show that the combination of waters and vegetated areas can mitigate effect of heat island effect, forming a strong cooling island effect (Morakinyo et al., 2013).

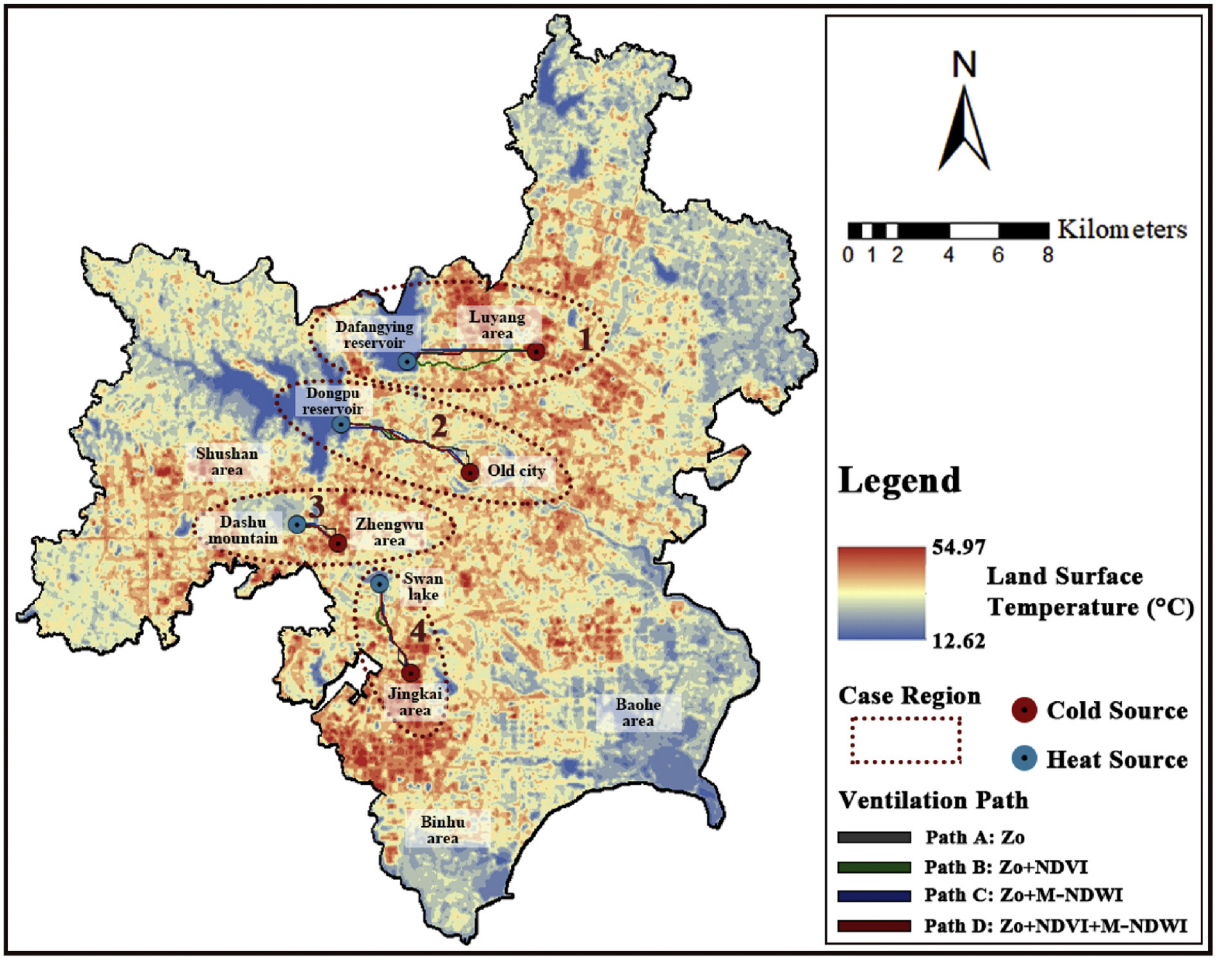

Fig. 7. Distribution of heat island effect intensity.

Table 3
Land surface temperature (LST) statistics in four areas under different paths.

Verification indicators	Regions	Cost indicators			
		Case A	Case B	Case C	Case D
		Z_0	Z_0+NDVI	Z_0+M-NDWI	Z_0+NDVI + M-NDWI
Average temperature(°C)	1	34.89	34.55	34.22	34.11
	2	32.21	31.91	31.85	31.73
	3	34.93	34.82	34.81	34.80
	4	35.45	35.38	35.21	34.93
Average value		34.37	34.17	34.02	33.89

5. Conclusion

Urban ventilation corridors can improve urban climate change, and the related planning needs to consider a variety of influencing factors, including adequate ventilation and wind benefits. In this paper, the least cost path LCP is used as the model to compare the ventilation corridors in multiple scenarios in Hefei (roughness, roughness + vegetated areas, roughness + waters, and roughness + vegetated areas + waters), combining urban heat island inversion with urban morphology. Through the comparison we can discover the optimal path for urban ventilation corridors. The main conclusions are as follows:

(1) The main urban area of Hefei exhibited relatively clear patterns of building heat source and ecological cold source. Above all, comprehensive assessment constructed based on LCP model could effectively optimize the ventilation corridors constructed based solely on urban morphological index.

(2) Different combinations of index showed different impacts on urban land surface ventilation, exhibiting the rule of land surface roughness < land surface roughness + vegetated areas < land surface roughness + waters < land surface roughness + vegetated areas + waters. Vegetated areas and waters could optimize urban ventilation and effectively reduce land surface temperature. Ventilation corridors constructed based on land surface roughness + vegetated areas + waters had the lowest temperature, and could generate the maximum of ventilation benefits.
(3) Waters had better efficiency on temperature reduction than vegetated areas on near-land surface level. Ventilation corridors constructed based on land surface roughness + waters had better capability of heat alleviation that based on land surface roughness + vegetated areas. Therefore, optimizing strategy of air quality should consider the spatial pattern of focusing more on waters while paying attention to vegetated areas.

Declaration of competing interest

The authors declared that they have no conflicts of interest to this work.

Acknowledgments

This research was funded by Natural Science Foundation of Anhui Province with the Grant reference No. 2008085ME160. We would like to thank the journal's editor and reviewers for their very useful comments, which greatly helped us to improve the paper; and to production editor for his support in the final proofreading of this publication.

References

Badas, M. G., Ferrari, S., Garau, M., & Querzoli, G. (2017). On the effect of gable roof on natural ventilation in two-dimensional urban canyons. *Journal of Wind Engineering and Industrial Aerodynamics, 162*, 24–34.
Bajsanski, I., Stojakovic, V., & Jovanovic, M. (2016). Effect of tree location on mitigating parking lot insolation. *Computers, Environment and Urban Systems, 56*, 59–67.
Bottema, M. (1997). Urban roughness modelling in relation to pollutant dispersion. *Atmospheric Environment, 31*(18), 3059–3075.
Bottema, M., & Mestayer, P. G. (1998). Urban roughness mapping-validation techniques and some first results. *Journal of Wind Engineering and Industrial Aerodynamics, 74*, 163–173.
Burian, S. J., Brown, M. J., & Linger, S. P. (2002). *Morphological analyses using 3D urban databases*. Los Angeles: Los Alamos National Laboratory.
Cariolet, J. M., Colombert, M., Vuillet, M., & Diab, Y. (2018). Assessing the resilience of urban areas to traffic-related air pollution: Application in Greater Paris. *The Science of the Total Environment, 615*, 588–596.
Coccolo, S., Kämpf, J., Scartezzini, J., & Pearlmutter, D. (2016). Outdoor human comfort and thermal stress: A comprehensive review onmodels and standards. *Urban Climate, 18*, 33–57.
Ding, C., Lam, K. P., & Feng, W. (2017). An evaluation index for cross ventilation based on CFD simulations and ventilation prediction model using machine learning algorithms. *Procedia Engineering, 205*, 2948–2955.
Du, H. Y. (2018). *The cool island effect of urban blue-green spaces and impact factors in mega city: A case study of Shanghai*. Shanghai: East China Normal University.
Edussuriya, P., Chan, A., & Ye, A. (2011). Urban morphology and air quality in dense residential environments in Hong Kong. Part I: District-level analysis. *Atmospheric Environment, 45*(27), 4789–4803.
Formica, A. E., Burnside, R. J., & Dolman, P. M. (2017). Rainfall validates MODIS-derived NDVI as an index of spatio-temporal variation in green biomass across non-montane semi-arid and arid Central Asia. *Journal of Arid Environments, 142*, 11–21.
Gál, T., & Sümeghy, Z. (2007). Mapping the roughness parameters in a large urbanarea for urban climate applications. *Acta Climatologica et Chorologica, 40*, 27–36.
Ghosh, M. K., Kumar, L., & Roy, C. (2015). Monitoring the coastline change of Hatiya Island in Bangladesh using remote sensing techniques. *ISPRS Journal of Photogrammetry and Remote Sensing, 101*, 137–144.
Guo, W., Liu, X., & Yuan, X. (2015). A case study on optimization of building design based on CFD simulation technology of wind environment. *Procedia Engineering, 121*, 225–231.
Hang, J., Li, Y., Sandberg, M., Buccolieri, R., & Di Sabatino, S. (2012). The influence of building height variability on pollutant dispersion and pedestrian ventilation in idealized high-rise urban areas. *Building and Environment, 56*, 346–360.
He, B. J. (2018). Potentials of meteorological characteristics and synoptic conditions to mitigate urban heat island effects. *Urban Climate, 24*, 26–33. https://doi.org/10.1016/j.uclim.2018.01.004
He, B. J., Ding, L., & Prasad, D. (2019). Enhancing urban ventilation performance through the development of precinct ventilation zones: A case study based on the greater Sydney, Australia. *Sustainable Cities and Society, 47*, 101472.
He, B. J., Ding, L., & Prasad, D. (2020a). Urban ventilation and its potential for local warming mitigation: A field experiment in an open low-rise gridiron precinct. *Sustainable Cities and Society, 55*, 102028. https://doi.org/10.1016/j.scs.2020.102028
He, B. J., Ding, L., & Prasad, D. (2020b). Wind-sensitive urban planning and design: Precinct ventilation performance and its potential for local warming mitigation in an open midrise gridiron precinct. *Journal of Building Engineering, 29*, 101145. https://doi.org/10.1016/j.jobe.2019.101145
Hong, B., & Lin, B. (2015). Numerical studies of the outdoor wind environment and thermal comfort at pedestrian level in housing blocks with different building layout patterns and trees arrangement. *Renewable Energy, 73*, 18–27.
Hsieh, C., & Huang, H. (2016). Mitigating urban heat islands: A method to identify potential wind corridor for cooling and ventilation. *Computers, Environment and Urban Systems, 57*, 130–143.
Huang, H. C., Lin, F. T., & Hsieh, C. M. (2014). A simple method for designation of urban ventilation path by using agent analyst in GIS — a study of Tainan, Taiwan. In *Conference on sustainable business, energy and development in Asia* (Hiroshima, Japan).
Huang, X., & Wang, Y. (2019). Investigating the effects of 3D urban morphology on the surface urban heat island effect in urban functional zones by using high-resolution remote sensing data: A case study of wuhan, Central China. *ISPRS Journal of Photogrammetry and Remote Sensing, 152*, 119–131.
Jan, F. C., Hsieh, C. M., Ishikawa, M., & Sun, Y. H. (2013). The influence of tree allocation and tree transpiration on the urban microclimate: An analysis of a subtropical urban park. *Environment and Urbanization ASIA, 4*(1), 135–150.
Kent, C. W., Grimmond, S., & Gatey, D. (2017). Aerodynamic roughness parameters in cities: Inclusion of vegetation. *Journal of Wind Engineering and Industrial Aerodynamics, 169*, 168–176.
Li, J., Deng, W., & Zhang, J. F. (2019b). Evaluating mountain water scarcity on the county scale: A case study of Dongchuan district, Kunming, China. *Journal of Mountain Science, 16*(4), 744–754.
Li, B., Jiang, C. Y., Wang, L., Cai, W. H., & Liu, J. (2019a). A parametric study of the effect of building layout on wind flow over an urban area. *Building and Environment*, 160.
Liu, S. M., Pan, W. X., & Cao, Q. (2019). CFD simulations of natural cross ventilation through an apartment with modified hourly wind information from a meteorological station. *Energy and Buildings, 195*, 16–25.

Liu, S. Y., & Shen, J. H. (2010). Urban ventilation channel planning method based on local circulation: A case study of Stuttgart, Germany. *Journal of Zhejiang University (Engineering Science), 44*(10), 1985–1991.
Liu, Y. H., Zhang, S., Cheng, P. F., Chen, P., Wei, L., & Fang, X. Y. (2017). Research and application of heat and ventilation environment assessment for city planning: A case study of Jinan central urban area. *Ecology and Environmental Sciences, 26*(11), 1892–1903.
Li, X. M., Zhou, W. Q., & Ouyang, Z. Y. (2013). Relationship between land surface temperature and spatial pattern of greenspace: What are the effects of spatial resolution? *Landscape and Urban Planning, 114*, 1–8, 0.
Luo, Y. W., He, J., & Ni, Y. L. (2017). Analysis of urban ventilation potential using rule-based modeling. *Computers, Environment and Urban Systems, 66*, 13–22.
Lyu, T., Buccolieri, R., & Gao, Z. (2015). A numerical study on the correlation between Sky view factor and summer microclimate of local climate zones. *Atmosphere, 10*, 8.
Marzena, W., Andreas, W., & Katarzyna, O. S. (2017). Detection of ventilation corridors using a spatio-temporal approach aided by remote sensing data. *European Journal of Remote Sensing, 50*(1), 254–267. https://doi.org/10.1080/22797254.2017.1318672
Marzena, W., & Katarzyna, O. S. (2016). Temporal analysis of urban changes and development in Warsaw's ventilation corridors. *Miscellanea Geographica, 20*(4), 11–21. https://doi.org/10.1515/mgrsd-2016-0021
Morakinyo, T. E., Balogun, A. A., & Adegun, O. B. (2013). Comparing the effect of trees on thermal conditions of two typical urban buildings. *Urban Climate, 3*, 76–93.
Oke, T. R. (1982). The energetic basis of the urban heat island. *Quarterly Journal of the Royal Meteorological Society, 108*(455), 1–24.
Qiao, Z., Xu, X. L., Wu, F., Luo, W., Wang, F., Liu, L., & Sun, Z. Y. (2017). Urban ventilation network model: A case study of the core zone of capital function in Beijing metropolitan area. *Journal of Cleaner Production, 168*, 526–535.
Rao, Y. H., Liang, S. L., Wang, D. D., Yu, Y. Y., Song, Z., Zhou, Y., Shen, M. G., & Xu, B. Q. (2019). Estimating daily average surface air temperature using satellite land surface temperature and top-of-atmosphere radiation products over the Tibetan Plateau. *Remote Sensing of Environment, 234*(1), 111462.
Sheng, L., Tang, X. L., You, H. Y., Gu, Q., & Hu, H. (2017). Comparison of the urban heat island intensity quantified by using air temperature and Landsat land surface temperature in Hangzhou, China. *Ecological Indicators, 72*, 738–746.
Stewart, I. D., & Oke, T. R. (2012). Local climate zones for urban temperature studies. *Bulletin of the American Meteorological Society, 93*(12), 1879–1900.
Vernay, D. G., Raphael, B., & Smith, lanF. C. (2015). Improving simulation predictions of wind around buildings using measurements through system identification techniques. *Building and Environment, 94*, 620–631.
Wang, X., Zhou, T., Tao, F., & Zang, F. Y. (2019). Correlation analysis between UBD and LST in Hefei, China, using Luojia1-01 night-time light imagery. *Applied Sciences, 9*(5224), 1–2. https://doi.org/10.3390/app9235224
Weng, Q. P., Zhang, H., Bao, H. X., Liu, J. G., & Wu, H. (2015). Study on ventilation channels of Nanjing city. *Science Technology and Engineering, 15*(11), 89–94.
Wen, C. Y., Juan, Y. H., & Yang, A. S. (2017). Enhancement of city breathability with half open spaces in ideal urban street canyons. *Building and Environment, 112*, 322–336.
Wong, M. S., Nichol, J. E., To, P. H., & Wang, J. Z. (2010). A simple method for designation of urban ventilation corridors and its application to urban heat island analysis. *Building and Environment, 48*(8), 1880–1889.
Wrobel-Niedzwiecka, I., Drozdowska, V., & Piskozub, J. (2019). Effect of drag coefficient formula choice on wind stress climatology in the North Atlantic and the European Arctic. *Oceanologia, 61*(3), 291–299.
Yim, S. H. L., Fung, J. C. H., & Ng, E. Y. Y. (2014). An assessment indicator for air ventilation and pollutant dispersion potential in an urban canopy with complex natural terrain and significant wind variations. *Atmospheric Environment, 94*, 297–306.
Yin, C. H., Yuan, M., Lu, Y. P., & Liu, Y. F. (2018). Effects of urban form on the urban heat island effect based on spatial regression model. *The Science of the Total Environment, 634*, 696–704.
Yuan, C., Ren, C., & Ng, E. (2014). GIS-based surface roughness evaluation in the planning system to improve the wind environment — a study in Wuhan, China. *Urban Climate, 10*(3), 585–593.
Zhang, Y. L., & Li, X. (2017). Study on urban ventilation channels planning based on optimization of the spatial layout in urban green space:a case study of Jinzhong. *Urban Development Studies, 24*, 35–41, 05.
Zheng, Y. T., Han, J. C., Huang, Y. F., Fassnacht, S. R., Xie, S., Lv, E. Z., & Chen, M. (2018). Vegetation response to climate conditions based on NDVI simulations using stepwise cluster analysis for the Three-River Headwaters region of China. *Ecological Indicators, 92*, 18–29.